JOC Article
pubs.acs.org/joc

Intramolecular $\pi-\pi$ Stacking Interactions in 2-Substituted *N*,*N*-Dibenzylaziridinium Ions and Their Regioselectivity in Nucleophilic Ring-Opening Reactions

Saron Catak,*[,†,§] Matthias D'hooghe,[‡] Norbert De Kimpe,[‡] Michel Waroquier,[†,§] and Veronique Van Speybroeck*[,†,§]

[†]*Center for Molecular Modeling, Ghent University, Technologiepark 903, B-9052 Zwijnaarde, Belgium,* [‡]*Department of Organic Chemistry, Faculty of Bioscience Engineering, Ghent University, Coupure Links 653, B-9000 Ghent, Belgium, and* [§]*QCMM-Alliance Ghent-Brussels, Belgium*

veronique.vanspeybroeck@ugent.be; saron.catak@ugent.be

Received November 23, 2009

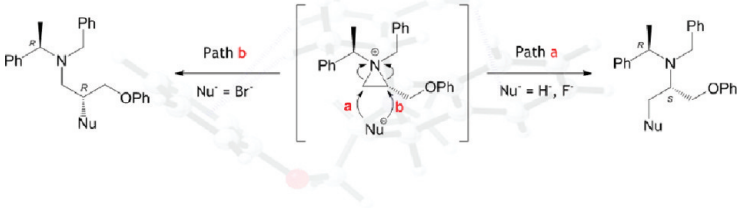

The ring opening of 2-substituted *N*,*N*-dibenzylaziridinium ions by bromide is known to occur exclusively at the substituted aziridine carbon atom via an S_N2 mechanism, whereas the opposite regioselectivity has been observed as the main pathway for ring opening by fluoride. Similarly, the hydride-induced ring opening of 2-substituted *N*,*N*-dibenzylaziridinium ions has been shown to take place solely at the less hindered position. To gain insight into the main factors causing this difference in regioselectivity, a thorough and detailed computational analysis was performed on the hydride- and halide-induced ring openings of 1-benzyl-1-(α-(*R*)-methylbenzyl)-2(*S*)-(phenoxymethyl)aziridinium bromide. Intramolecular $\pi-\pi$ stacking interactions in the aziridinium system were investigated at a range of levels that enable a proper description of dispersive interactions; a T-stacking conformer was found to be the most stable. Ring-opening mechanisms were investigated with a variety of DFT and high level *ab initio* methods to test the robustness of the energetics along the pathway in terms of the electronic level of theory. The necessity to utilize explicit solvent molecules to solvate halide ions was clearly shown; the potential energy surfaces for nonsolvated and solvated cases differed dramatically. It was shown that in the presence of a kinetically viable route, product distribution will be dictated by the energetically preferred pathway; this was observed in the case of hard nucleophiles (both hydride donors and fluoride). However, for the highly polarizable soft nucleophile (bromide), it was shown that in the absence of a large energy difference between transition states leading to competing pathways, the formation of the thermodynamic product is likely to be the driving force. Distortion/interaction analysis on the transition states has shown a considerable difference in interaction energies for the solvated fluoride case, pointing to the fact that sterics plays a major role in the outcome, whereas for the bromide this difference was insignificant, suggesting bromide is less influenced by the difference in sterics.

Introduction

The aziridine moiety represents one of the most valuable three-membered ring systems in organic chemistry as a result of its versatility as a building block for the preparation of a variety of (a)cyclic amines.[1−9] Although the chemistry of

(1) Lindström, U. M.; Somfai, P. *Tetrahedron Lett.* **1998**, *39*, 7173.

DOI: 10.1021/jo902493w Published on Web 12/29/2009

SCHEME 1. Nucleophilic Ring-Opening Reactions of Intermediate Aziridinium Ions 2 at the Unhindered (Pathway a) and Hindered (Pathway b) Aziridine Carbons

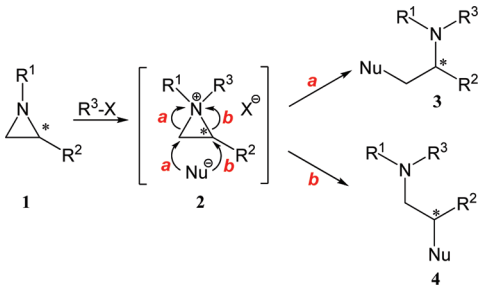

activated aziridines has been studied extensively in the past,[4] very little attention has been devoted to the utility of nonactivated aziridines in organic synthesis. Since the latter require activation toward aziridinium intermediates prior to ring opening, the reactivity and applications are often different when compared to activated aziridines. As depicted in Scheme 1, the nucleophilic ring opening of 2-substituted aziridinium ions **2**, prepared by *N*-alkylation of nonactivated aziridines **1**, can lead to two different ring-opening products. Ring opening can occur at the least hindered position (pathway a), leading to α-branched amines **3** in which the stereochemistry of the substituted aziridine carbon atom remains intact. Alternatively, ring opening can take place at the more hindered position (pathway b), affording 1-aminoalkanes **4** as the reaction products. In the latter case, the chiral center at C2 can either be inverted, if the reaction proceeds via an S_N2 protocol, or racemized, if a first order substitution reaction is involved (S_N1).

As *β*-haloamines comprise a synthetically useful class of compounds, many efforts are devoted to the development of new entries toward these reactive synthons.[10] The straightforward transformation of 1-arylmethyl-2-(alkoxymethyl)-aziridines **5** into the corresponding 3-amino-2-bromopropanes **6**, upon treatment with 1 equiv of an arylmethyl bromide in acetonitrile, has been previously reported.[11−15] This remarkable methodology was shown to proceed in a complete regio- and stereoselective manner through ring opening of intermediate aziridinium ions **8** by bromide at the substituted aziridinium carbon atom (Scheme 2).[12] In contrast, the ring opening of the same type of aziridinium ions **8** by fluoride in acetonitrile resulted in *β*-fluoroamines **7** as the major reaction product (72−86%), through ring opening at the less hindered aziridine carbon atom (Scheme 2, TBAF = tetrabutylammonium fluoride), as well as a minor amount of the counter regioisomers (14−28%).[16]

Recently, the reactivity of chiral *β*-bromoamines **10**, prepared through regiospecific ring opening of aziridinium ions **12** by bromide, with regard to hydride reagents has been investigated, pointing to a complete shift in regioselectivity as compared to ring opening of the aziridinium ions by bromide. Thus, treatment of (*R*)-3-amino-2-bromo-1-phenoxypropanes **10** with 3 equiv of sodium borohydride in THF furnished enantiopure (*S*)-2-amino-1-phenoxypropanes **11** as the sole reaction product through initial formation of intermediate aziridinium ions **12** and subsequent ring opening by hydride at the least hindered aziridine carbon atom (Scheme 3).[17]

The study of aziridinium ions **2** for regio- and stereoselective ring-opening reactions is a challenging fundamental topic, and the effect of substituents, nucleophiles, electrophiles, and solvents on the reaction outcome still remains largely unclear. Previous theoretical and experimental studies often consider one particular nucleophile and substrate, which makes a detailed understanding of the driving factors difficult. This study aims to shed light on the role of the nucleophile by considering two hydride donors (borohydride and aluminum hydride) and two halides (fluoride and bromide). For this purpose, nucleophilic ring-opening reactions of 2-substituted *N*,*N*-dibenzylaziridinium ions **12** will be evaluated theoretically. Previous computational work involved bromide-[12,14] and borohydride-mediated ring opening of aziridinium ions;[17] however, further analysis is required to identify the reasoning behind the experimentally observed regioselectivities and assess the reliability of the level of theory. Moreover, the substrates bear various aromatic functionalities, which can exhibit various conformations as a result of intramolecular *π*−*π* stacking interactions. A set of various DFT functionals, including empirical corrections for van der Waals interactions and post Hartree−Fock methods, were used to get a thorough and robust understanding of the various factors governing the reaction and the reactive intermediates. To the best of our knowledge, intramolecular *π*−*π* stacking in these systems has not yet been studied and is of particular interest in this study.

Computational Methods

Aziridinium ion **12** (R = Ph) conformers were optimized at the MP2/6-31+G(d) level of theory.[18] MP2 energies were further refined via Grimme's Spin-Component-Scaled (SCS) MP2 treatment,[19] which provides a uniform improvement over standard MP2 by individually scaling for the parallel (scaled by 1/3) and antiparallel (scaled by 6/5) pair electron correlation energies. Relative stabilities of conformers were investigated via single-point energy calculations with a range of DFT functionals. Hybrid GGA B3LYP,[20,21] PBE0,[22] and BMK;[23]

(2) Zwanenburg, B.; ten Holte, P. *Top. Curr. Chem.* **2001**, *216*, 93.
(3) Sweeney, J. B. *Chem. Soc. Rev.* **2002**, *31*, 247.
(4) Hu, X. E. *Tetrahedron* **2004**, *60*, 2701.
(5) Tanner, D. *Angew. Chem., Int. Ed. Engl.* **1994**, *33*, 599.
(6) Osborn, H. M. I.; Sweeney, J. *Tetrahedron: Asymmetry* **1997**, *8*, 1693.
(7) Coull, W. M.; Davis, F. A. *Synthesis* **2000**, 1347.
(8) Watson, I. D. G.; Yu, L.; Yudin, A. K. *Acc. Chem. Res.* **2006**, *39*, 194.
(9) Padwa, A.; Murphree, S. S. *Arkivoc* **2006**, *iii*, 6.
(10) D'hooghe, M.; De Kimpe, N. *Tetrahedron* **2008**, *64*, 3275.
(11) D'hooghe, M.; Van Brabandt, W.; De Kimpe, N. *J. Org. Chem.* **2004**, *69*, 2703.
(12) D'hooghe, M.; Van Speybroeck, V.; Waroquier, M.; De Kimpe, N. D. *Chem. Commun.* **2006**, 1554.
(13) D'hooghe, M.; Waterinckx, A.; Vanlangendonck, T.; De Kimpe, N. *Tetrahedron* **2006**, *62*, 2295.
(14) D'hooghe, M.; Van Speybroeck, V.; Van Nieuwenhove, A.; Waroquier, M.; De Kimpe, N. *J. Org. Chem.* **2007**, *72*, 4733.
(15) D'hooghe, M.; Vervisch, K.; De Kimpe, N. *J. Org. Chem.* **2007**, *72*, 7329.
(16) D'hooghe, M.; De Kimpe, N. *Synlett* **2006**, *13*, 2089.
(17) Yun, S. Y.; Catak, S.; Lee, W. K.; D'hooghe, M.; De Kimpe, N. D.; Van Speybroeck, V.; Waroquier, M.; Kim, Y.; Ha, H.-J. *Chem. Commun.* **2009**, 2508.
(18) Møller, C.; Plesset, M. S. *Phys. Rev.* **1934**, *46*, 618.
(19) Gerenkamp, M.; Grimme, S. *Chem. Phys. Lett.* **2004**, *392*, 229.
(20) Lee, C.; Yang, W.; Parr, R. G. *Phys. Rev. B* **1988**, *37*, 785.
(21) Becke, A. D. *J. Chem. Phys.* **1993**, *98*, 5648.
(22) Adamo, C.; Barone, V. *J. Chem. Phys.* **1999**, *110*, 6158.
(23) Boese, A. D.; Martin, J. M. L. *J. Chem. Phys.* **2004**, *121*, 3405.

SCHEME 2. Bromide- and Fluoride-Induced Regioselective Ring-Opening Reactions of Intermediate Aziridinium Ions 8

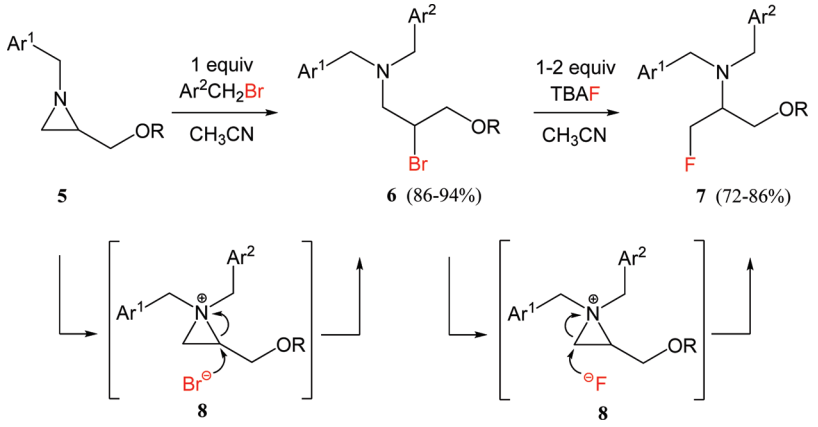

SCHEME 3. Hydride-Induced Regioselective Ring-Opening Reactions of Intermediate Aziridinium Ions 12

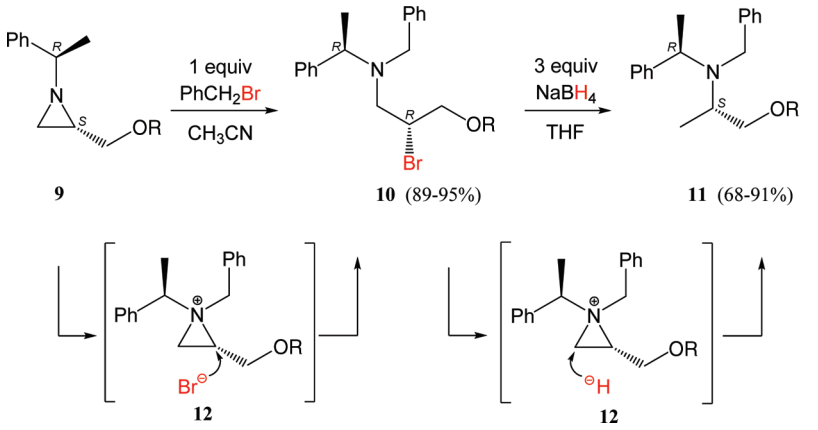

meta-hybrid GGA MPW1B95[24] and M06-2X;[25,26] and double-hybrid GGA B2-PLYP[27] functionals were used. The DFT-D[28] approach, which has proven to be a cost-efficient and accurate alternative to empirically add long-range dispersive corrections and account for van der Waals (vdW) interactions, was applied in conjunction with hybrid GGAs B3LYP and PBE0, to take into account possible $\pi-\pi$ stacking interactions in the aziridinium system under study. The effect of the solvent environment on conformers of aziridinium ion **12** was also taken into account by means of self-consistent reaction field (SCRF) theory.[29] Solvation free energies in acetonitrile (MeCN, ε = 36.6) were obtained via the conductor-like polarizable continuum model (C-PCM).[30,31] PAULING atomic radii (with explicit hydrogen spheres) were used. A CPCM benchmarking study by Houk[32] has shown PAULING cavities to reproduce experimental solvation free energies in ionic systems quite efficiently.

Reaction pathways for the nucleophilic attack of halides and hydrides on aziridinium ion **12** were obtained using B3LYP and MPW1B95 functionals with a 6-31++G(d,p) basis set. Explicit acetonitrile molecules were used to solvate halide ions. Stationary points were characterized as minima or first-order saddle points via frequency calculations. Intrinsic reaction coordinate (IRC)[33] calculations followed by full geometry optimizations were used to verify reactant complexes (ion-dipole complex) and products reached by each transition state. Energies were further refined via MP2, SCS-MP2, B2-PLYP, PBE0, BMK, and B3LYP-D single-point calculations. All *ab initio* and DFT calculations were carried out with the Gaussian 03 program package;[34] DFT-D and M06-2X single-point calculations were performed utilizing the ORCA 2.6.35[35] and NWCHEM 5.1.1[36,37] software packages, respectively.

Results and Discussion

To rationalize the differences in regioselectivities, a thorough and detailed computational analysis was performed on the hydride- and halide-induced ring opening of 1-benzyl-1-(α(*R*)-methylbenzyl)-2(*S*)-(phenoxymethyl)aziridinium bromide.

(24) Zhao, Y.; Truhlar, D. G. *J. Phys. Chem. A* **2004**, *108*, 6908.
(25) Zhao, Y.; Truhlar, D. G. *Acc. Chem. Res.* **2008**, *41*, 157.
(26) Zhao, Y.; Truhlar, D. *Theor. Chim. Acta* **2008**, *120*, 215.
(27) Schwabe, T.; Grimme, S. *Phys. Chem. Chem. Phys.* **2007**, *9*, 3397.
(28) Grimme, Stefan *J. Comput. Chem.* **2004**, *25*, 1463.
(29) Tomasi, J.; Mennucci, B.; Cammi, R. *Chem. Rev.* **2005**, *105*, 2999.
(30) Barone, V.; Cossi, M. *J. Phys. Chem. A* **1998**, *102*, 1995.
(31) Cossi, M.; Rega, N.; Scalmani, G.; Barone, V. *J. Comput. Chem.* **2003**, *24*, 669.
(32) Takano, Y.; Houk, K. N. *J. Chem. Theory Comput.* **2004**, *1*, 70.
(33) Fukui, K. *Acc. Chem. Res.* **2002**, *14*, 363.
(34) Frisch, M. J. et al. *Gaussian 03, Revision C.02*; Gaussian, Inc.: Wallingford, CT, 2004.
(35) ORCA. 2.6.35 ed.; http://www.thch.uni-bonn.de/tc/orca/.
(36) Bylaska, E. J. et al. *A Computational Chemistry Package for Parallel Computers*, Version 5.1; Pacific Northwest National Laboratory: Richland, WA, 2007.
(37) Kendall, R. A.; Apra, E.; Bernholdt, D. E.; Bylaska, E. J.; Dupuis, M.; Fann, G. I.; Harrison, R. J.; Ju, J.; Nichols, J. A.; Nieplocha, J.; Straatsma, T. P.; Windus, T. L.; Wong, A. T. *Comput. Phys. Commun.* **2000**, *128*, 260.

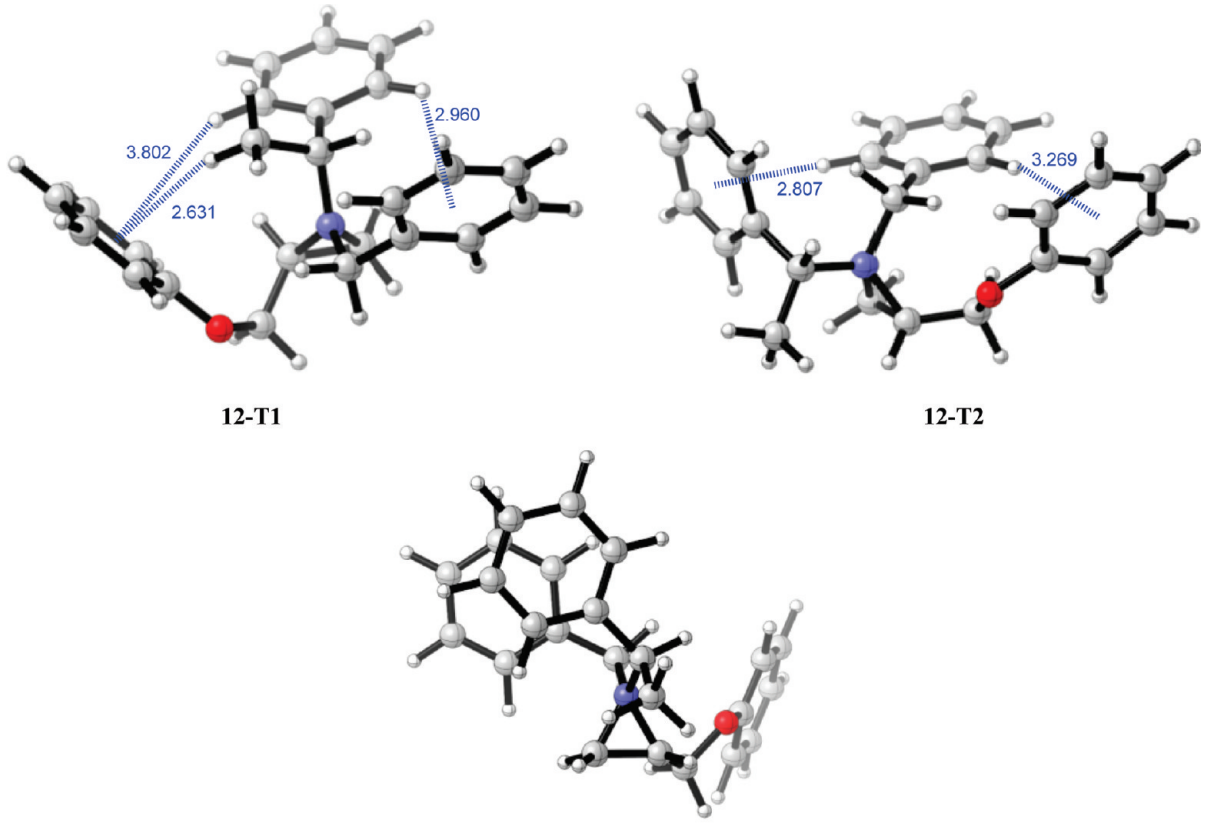

FIGURE 1. Aziridinium conformers optimized at the MP2/6-31+G(d) level of theory. Some critical distances (Å) are given.

TABLE 1. Relative Electronic Energies (kJ/mol) of Aziridinium Conformers

method[a]	12-PD	12-T1	12-T2
MP2/6-31++G(d,p)//MP2/6-31+G(d)	29.3	0.0	14.4
B3LYP/6-31++G(d,p)//B3LYP/6-31++G(d,p)	n/a	0.0	7.6
MPW1B95/6-31++G(d,p)//MPW1B95/6-31++G(d,p)	n/a	0.0	8.6
SCS-MP2/6-31++G(d,p)//MP2/6-31+G(d)	28.1	0.0	12.3
B2-PLYP/TZVP//MP2/6-31+G(d)	29.2	0.0	8.0
B3LYP/6-31++G(d,p)//MP2/6-31+G(d)	28.9	0.0	4.3
B3LYP-D/6-31++G(d,p)//MP2/6-31+G(d)	35.9	0.0	13.2
MPW1B95/6-31++G(d,p)//MP2/6-31+G(d)	33.4	0.0	9.6
PBE0/6-31++G(d,p)//MP2/6-31+G(d)	32.3	0.0	7.2
PBE0-D/6-31++G(d,p)//MP2/6-31+G(d)	37.4	0.0	13.5
BMK/6-31++G(d,p)//MP2/6-31+G(d)	33.2	0.0	10.4
M06-2X/6-31++G(d,p)//MP2/6-31+G(d)	31.1	0.0	12.1

[a] $x//y$ represents the level of theory (LOT); x = LOT for energy; y = LOT for geometry.

Conformational analysis of aziridinium ion **12** was initially carried out to identify the most plausible conformer, which will later be used to model the nucleophilic attack mechanisms. Intramolecular stacking interactions within the substrate were investigated in detail.

Aziridinium Conformers and Intramolecular $\pi-\pi$ Stacking. Conformational analysis (MP2/6-31+G(d)) of the aziridinium ion, taking into account possible π-interactions among the three aryl entities within the compound, revealed three major conformers. One parallel-displaced $\pi-\pi$ interaction (**12-PD**) and two T-stacking (edge-to-face) π-interactions (**12-T1** and **12-T2**) were identified (Figure 1) with regard to the nonbonded interactions between the aromatic rings. All three conformations were initially optimized at the MP2/6-31+G(d) level of theory and further optimized with hybrid DFT functionals B3LYP and MPW1B95 (6-31++G(d,p) to verify the reproducibility of geometries and in particular $\pi-\pi$ stacking interactions. Although MP2 calculations successfully accounted for a $\pi-\pi$ stacking interaction leading to the parallel-displaced **12-PD** conformation, DFT's inherent deficiency to account for dispersion failed to identify this aromatic interaction, and hence the off-centered parallel orientation **12-PD** was not located at the DFT levels B3LYP/6-31++G(d,p) and MPW1B95 (6-31++G(d,p) (Table 1). However, both hybrid functionals reproduced **12-T1** and **12-T2** geometries as well as relative stabilities quite efficiently. Relative energies of conformers at various levels of theory are given in Table 1. Single-point DFT calculations—including Grimme's double hybrid functional B2-PLYP, known to provide highly accurate results over a

wide range of properties,[27,38] and Truhlar's newly developed density functional M06-2X, recently shown to correctly predict $\pi-\pi$ stacking interactions[39] —were performed on MP2 geometries, to properly identify the most plausible conformer for aziridinium ion **12**. Although MP2 qualitatively reproduces accurate PES data for stacked complexes,[40] it is well-known to consistently overestimate binding energies, and hence MP2 energies were further refined with Grimme's SCS-MP2 treatment. In addition, DFT-D corrections were applied on B3LYP and PBE0 energies to account for dispersive interactions.

Relative energies of aziridinium conformers at the MP2 level depict (Table 1) **12-T1**, which embodies a number of favorable C−H$\cdots\pi$ interactions (Figure 1) including a $CH_3\cdots\pi$ interaction, as the most stable of the three conformers. Figure 1 depicts a slight difference in C−H$\cdots\pi$ distances among the two T-shaped conformers, which accordingly accounts for the difference in stabilities. The **12-PD** conformer is shown (Figure 1) to bear a $\pi-\pi$ stacking interaction; the parallel-displaced (displaced at 17.1°) aromatic rings on the N-substituents are sufficiently close (3.559 Å from center to center) to give rise to a favorable interaction. These distances are in accord with typical T-stacking and parallel-displaced geometries reported in the literature,[40−43] which range between 3.5 and 4.0 Å. However, the two T-stacked conformers are shown to be more stable than **12-PD**. DFT single-point calculations, performed on MP2/6-31+G(d) geometries, reveal the same trend in conformer stability; **12-T1** being the most stable followed by a small difference in energy by **12-T2** and **12-PD** being the least stable of the three (Table 1). DFT-D corrections, in conjunction with the B3LYP and PBE0 functionals, performed notably in comparison to MP2 and SCS-MP2, which has also verified **12-T1** as the most predominant geometry for aziridinium ion **12**. M06-2X results are also consistent with SCS-MP2 energies.

Aromatic $\pi-\pi$ stacking interactions have been subject to many computational studies,[39,41,42,44−50] and recent advances in theoretical methodologies[24,26−28,38,45,51,52] that can account for these dispersive interactions have gained considerable interest. Recent computational studies on aromatic dimers have shown T-shaped and parallel-displaced configurations to be nearly isoenergetic and slightly more stable than the face-to-face sandwich configuration.[40,43,53] The effect of substituents on $\pi-\pi$ interactions have also been subject to theoretical work, and although all substituted sandwich dimers, regardless of electron-withdrawing or -donating character, were shown to bind stronger than the parent benzene dimer, binding aptitude in T-shaped configurations was dependent on the identity of the substituent. Electron-donating substituents that increase electron density in the ring, such as alkyl groups, lead to more favorable dispersion energies in the T-shaped configurations,[43,53] as in the case of the aziridinium ion **12** conformers under study.

TABLE 2. Molecular Dipole Moment (debye) and Relative Electronic (E_{rel}) and Solvation Free (G_{rel}) Energies (kJ/mol) of Aziridinium Conformers[a]

		CPCM (ε = 36.6) MPW1B95/6-31++G(d,p)	
	μ	E_{rel}	G_{rel}[b]
12-PD	4.51	22.8	22.5
12-T1	3.41	0.0	0.0
12-T2	4.26	9.5	8.6

[a]MP2/6-31+G(d) geometries. [b]All nonelectrostatic terms included.

TABLE 3. Atomic Charges on 12-T1 Ring Carbons

	Mulliken[a]		NPA		CHELPG	
	C2	C3	C2	C3	C2	C3
B3LYP/	+0.66	−0.41 (−0.02)			+0.05	
6-31++G(d,p)	(+0.85)		−0.08	−0.21		−0.15
MPW1B95/	+0.85	−0.51 (−0.06)			+0.03	
6-31++G(d,p)	(+0.99)		−0.09	−0.22		−0.17
MP2/	+0.20	−0.099			+0.07	
6-31++G(d,p)	(+0.34)	(+0.29)	−0.04	−0.16		−0.17

[a]Mulliken charges with hydrogens summed into heavy atoms given in brackets.

TABLE 4. Summary of Experimental Regioselectivities (%) in the Ring Opening of Aziridinium Ions for Various Nucleophiles[11−17]

	nucleophile			
	BH_4^-	AlH_4^-	F^-	Br^-
pathway a (unhindered)	68−91%	20−40%[a]	72−86%	
pathway b (hindered)				86−94%

[a]Side product *N*-allyl-*N*-benzyl-*N*-(1-phenylethyl)amine obtained in 23−36% yield.

The effect of the solvent environment on aziridine conformer stabilities was accounted for by means of a dielectric continuum (MeCN, ε = 36.6). As depicted in Table 2, relative stability of **12-PD** has improved considerably. CPCM energies correlate well with gas-phase results in terms of relative stabilities of the aziridinium conformers, depicting **12-T1** as the most plausible conformer. As such, further mechanistic investigations on the nucleophile-induced ring-opening reactions of aziridinium ion **12** will be performed using the aziridinium ion in the **12-T1** geometry.

Mulliken,[54] NPA,[55] and CHELPG[56] atomic charges for **12-T1** ring carbons C2 and C3 are listed in Table 3. All three methods indicate a preference of nucleophilic attack at C2, which is clearly more positively charged than C3. However,

(38) Schwabe, T.; Grimme, S. *Acc. Chem. Res.* **2008**, *41*, 569.
(39) Gu, J.; Wang, J.; Leszczynski, J.; Xie, Y.; Schaefer, H. F., III. *Chem. Phys. Lett.* **2008**, *459*, 164.
(40) Sinnokrot, M. O.; Sherrill, C. D. *J. Phys. Chem. A* **2004**, *108*, 10200.
(41) Podeszwa, R.; Bukowski, R.; Szalewicz, K. *J. Phys. Chem. A* **2006**, *110*, 10345.
(42) Waller, M. P.; Robertazzi, A.; Platts, J. A.; Hibbs, D. E.; Williams, P. A. *J. Comput. Chem.* **2006**, *27*, 491.
(43) Sinnokrot, M. O.; Sherrill, C. D. *J. Am. Chem. Soc.* **2004**, *126*, 7690.
(44) Zhao, Y.; Truhlar, D. G. *Phys. Chem. Chem. Phys.* **2005**, *7*, 2701.
(45) Grimme, S.; Antony, J.; Schwabe, T.; Muck-Lichtenfeld, C. *Org. Biomol. Chem.* **2007**, *5*, 741.
(46) Piacenza, M.; Grimme, S. *J. Comput. Chem.* **2004**, *25*, 83.
(47) McGaughey, G. B.; Gagne, M.; Rappe, A. K. *J. Biol. Chem.* **1998**, *273*, 15458.
(48) Morgado, C.; Vincent, M. A.; Hillier, I. H.; Shan, X. *Phys. Chem. Chem. Phys.* **2007**, *9*, 448.
(49) Pavone, M.; Rega, N.; Barone, V. *Chem. Phys. Lett.* **2008**, *452*, 333.
(50) Zhao, Y.; Truhlar, D. G. *J. Chem. Theory Comput.* **2006**, *2*, 1009.
(51) Benighaus, T.; DiStasio, R. A.; Lochan, R. C.; Chai, J.-D.; Head-Gordon, M. *J. Phys. Chem. A* **2008**, *112*, 2702.
(52) Schwabe, T.; Grimme, S. *Phys. Chem. Chem. Phys.* **2006**, *8*, 4398.
(53) Sinnokrot, M. O.; Sherrill, C. D. *J. Phys. Chem. A* **2003**, *107*, 8377.
(54) Mulliken, R. S. *J. Chem. Phys.* **1955**, *23*, 1833.
(55) Reed, A. E.; Weinstock, R. B.; Weinhold, F. *J. Chem. Phys.* **1985**, *83*, 735.
(56) Breneman, Curt M.; Wiberg, K. B. *J. Comput. Chem.* **1990**, *11*, 361.

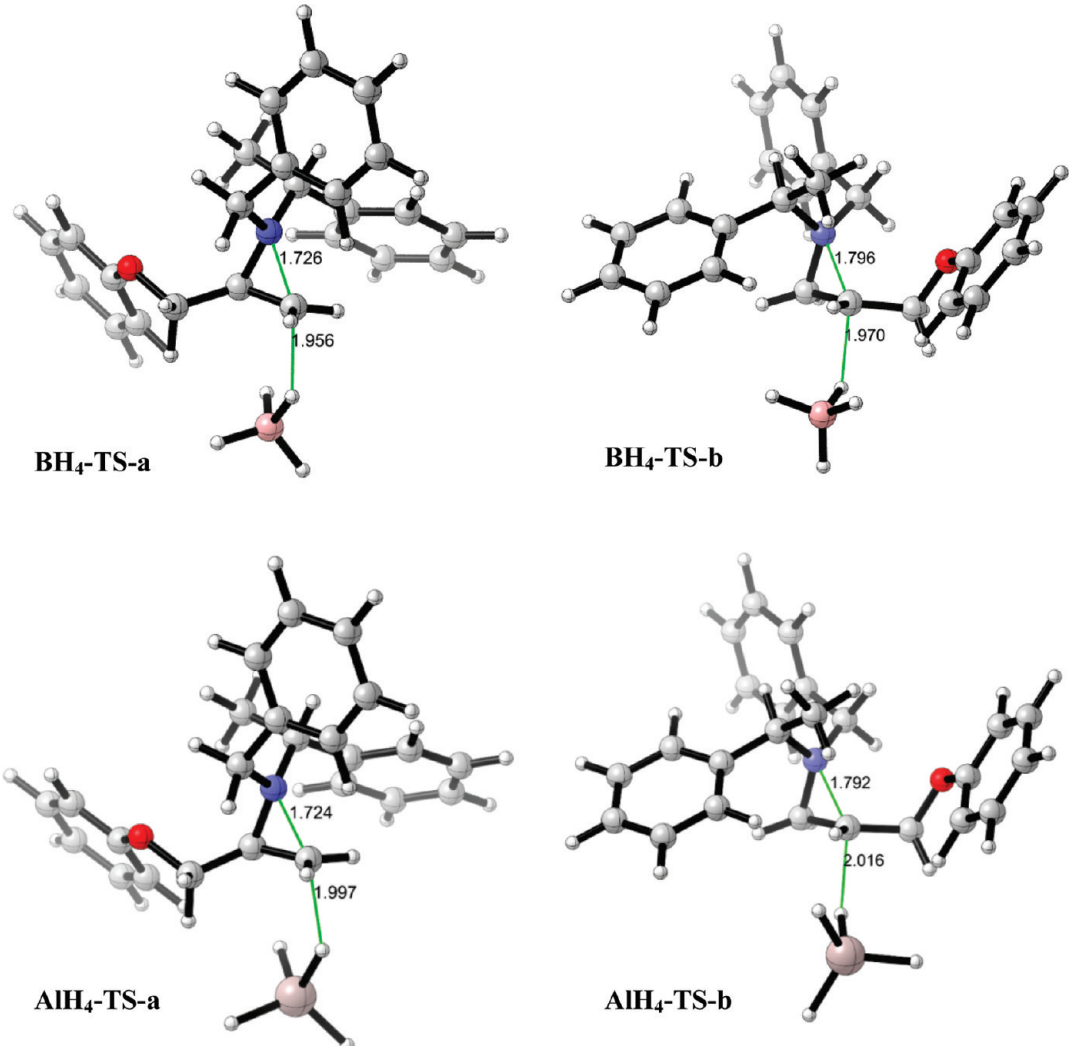

FIGURE 2. Transition state geometries optimized at the B3LYP/6-31++G(d,p) level of theory for BH_4^-- and AlH_4^--induced ring-opening reactions of aziridinium ion **12-T1** via pathways a and b, respectively. Some critical distances (Å) are given.

steric effects, nucleophile strength, nucleophile attack trajectories, distortion/interaction energies, and barrier heights will all play a role in understanding the ultimate outcome of the aziridinium nucleophilic ring-opening reactions.

Nucleophilic Ring-Opening Mechanisms. This study aims to rationalize experimental regioselectivities observed for the hydride- and halide-induced regioselective ring-opening reactions of the aziridinium ion **12-T1** (Figure 1). For this purpose two competing pathways were modeled: attack at the unhindered (pathway a) and hindered (pathway b) aziridine carbon (Scheme 1). Experimental results have shown that hydride (both BH_4^- and AlH_4^-) and fluoride attacks have a preference for the sterically less hindered unsubstituted carbon C3 as expected for S_N2-type reactions, whereas bromide-induced ring opening afforded the counter regioisomer, suggesting a preference of attack on the hindered carbon C2. An overview of experimentally observed regioselectivities is given in Table 4. Both reaction pathways were modeled for each nucleophile via B3LYP/6-31++G(d,p) and MPW1B95/6-31++G(d,p) full geometry optimizations, which gave similar geometries, energies were further refined by single-point energy calculations with a range of DFT and *ab initio* methods. Consequent comparison of reaction barriers and relative stabilities of products will help understand the factors controlling regioselectivity for various nucleophiles.

Prior to the detailed discussion of nucleophilic ring-opening mechanisms of aziridinium ions, some general remarks on the reaction mechanism are in order. The nature of the potential energy surface (PES) of bimolecular nucleophilic substitution (S_N2) reactions has been extensively studied both experimentally and theoretically over the past few decades.[57] The double-well PES for gas-phase S_N2 reactions is known to consist of reactant and product complexes (ion-dipole complexes) that are deep minima, joined by a central transition state; isolated reactants are often higher in energy than the transition state. Consequently, in the present study, relative energies are reported with respect to the reactant-complex rather than the separated reactants. In nucleophilic ring-opening reactions, the leaving group is not a separate entity but part of the substrate; therefore there is no product

(57) Mikosch, J.; Trippel, S.; Eichhorn, C.; Otto, R.; Lourderaj, U.; Zhang, J. X.; Hase, W. L.; Weidemuller, M.; Wester, R. *Science* **2008**, *319*, 183.

TABLE 5. Relative Electronic Energies (kJ/mol) of Stationary Points along the Reaction Coordinate for Hydride-Induced Nucleophilic Ring Opening of 12-T1 via Pathways a (Unhindered) and b (Hindered)[a,b]

	BH_4^-					AlH_4^-				
method	RC	TS-a	TS-b	PC-a	PC-b	RC	TS-a	TS-b	PC-a	PC-b
B3LYP/6-31++G(d,p)	0.0	21.3	34.4	−192.7	−185.9	0.0	16.8	31.3	−223.0	−215.5
B3LYP-D/6-31++G(d,p)	0.0	23.4	36.6	−169.2	−158.2	0.0	17.2	31.4	−206.7	−194.7
MPW1B95/6-31++G(d,p)	0.0	34.4	47.0	−159.0	−149.8	0.0	28.4	44.2	−198.9	−190.3
PBE0/6-31++G(d,p)	0.0	28.0	42.3	−170.4	−163.0	0.0	22.4	38.6	−210.6	−202.6
BMK/6-31++G(d,p)	0.0	27.5	42.0	−177.1	−164.2	0.0	21.3	38.3	−216.3	−205.0
MP2/6-31++G(d,p)	0.0	35.5	48.7	−179.2	−158.1	0.0	29.3	47.1	−212.7	−194.2
SCS-MP2/6-31++G(d,p)	0.0	35.4	48.6	−191.6	−172.2	0.0	30.1	47.7	−216.4	−199.8
B2-PLYP/TZVP/	0.0	26.7	40.2	−190.1	−177.5	0.0	21.5	37.2	−221.4	−210.5

[a]B3LYP/6-31++G(d,p) geometries. [b]RC, TS, and PC represent reactive complex, transition state, and product complex (product-AlH_3 or product-BH_3), respectively.

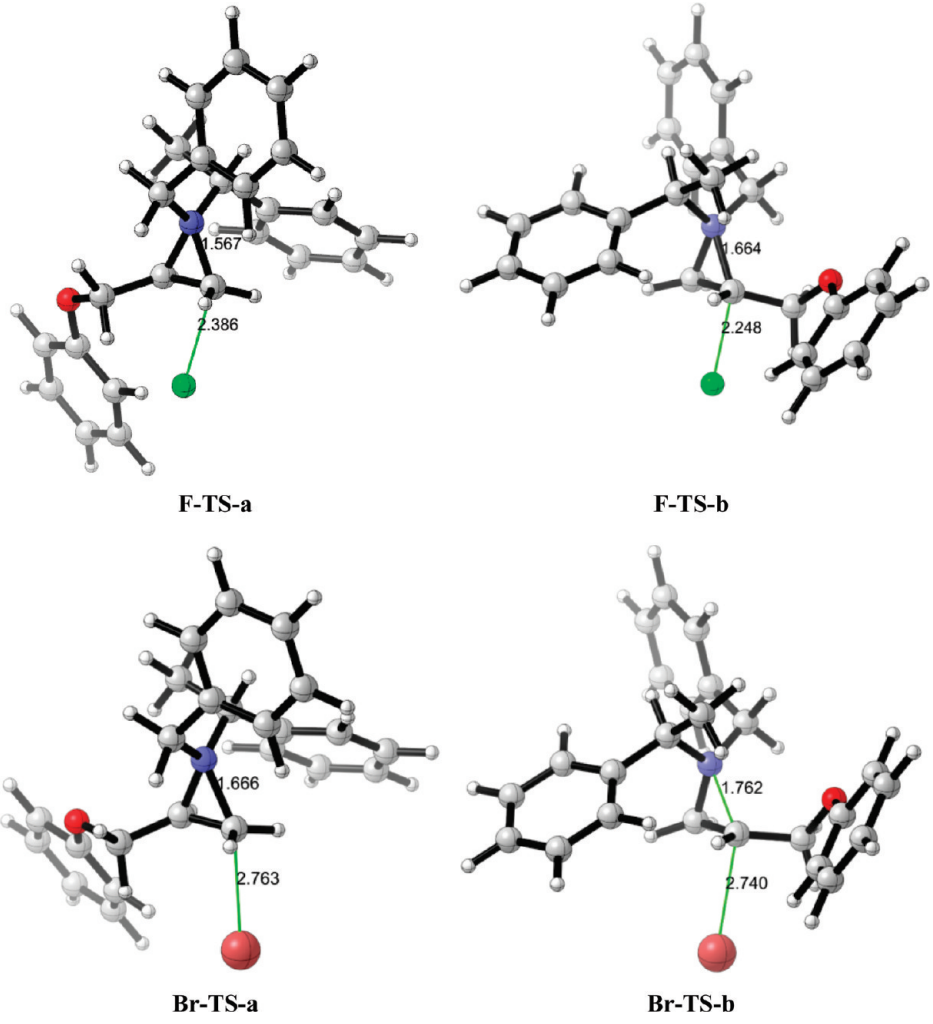

FIGURE 3. Transition state geometries optimized at the B3LYP/6-31++G(d,p) level of theory for halide-induced nucleophilic ring opening of aziridinium ion **12-T1**, without explicit solvent, through pathways a and b. Some critical distances are given in units of Å.

complex disintegration but a single end product, as is the case herein.

Recent theoretical studies have explored the important role sterics plays in the outcome of S_N2 reactions; however, the effect of the environment is also known to be undeniable.[58] Nucleophilic substitution reactions are well-known to be influenced by the solvent environment, and accordingly, previous computational studies on bromide-induced ring opening of aziridinium ions were shown to benefit from the use of explicit solvent molecules.[12,14] In light of this, the current study focused on modeling the halide-induced ring-opening reaction of aziridinium ions, which was previously theoretically verified to have a bimolecular nature, taking into account the reactive species as well as explicit solvent molecules that effectively solvate the halide ion. This study

(58) Vayner, G.; Houk, K. N.; Jorgensen, W. L.; Brauman, J. I. *J. Am. Chem. Soc.* **2004**, *126*, 9054.

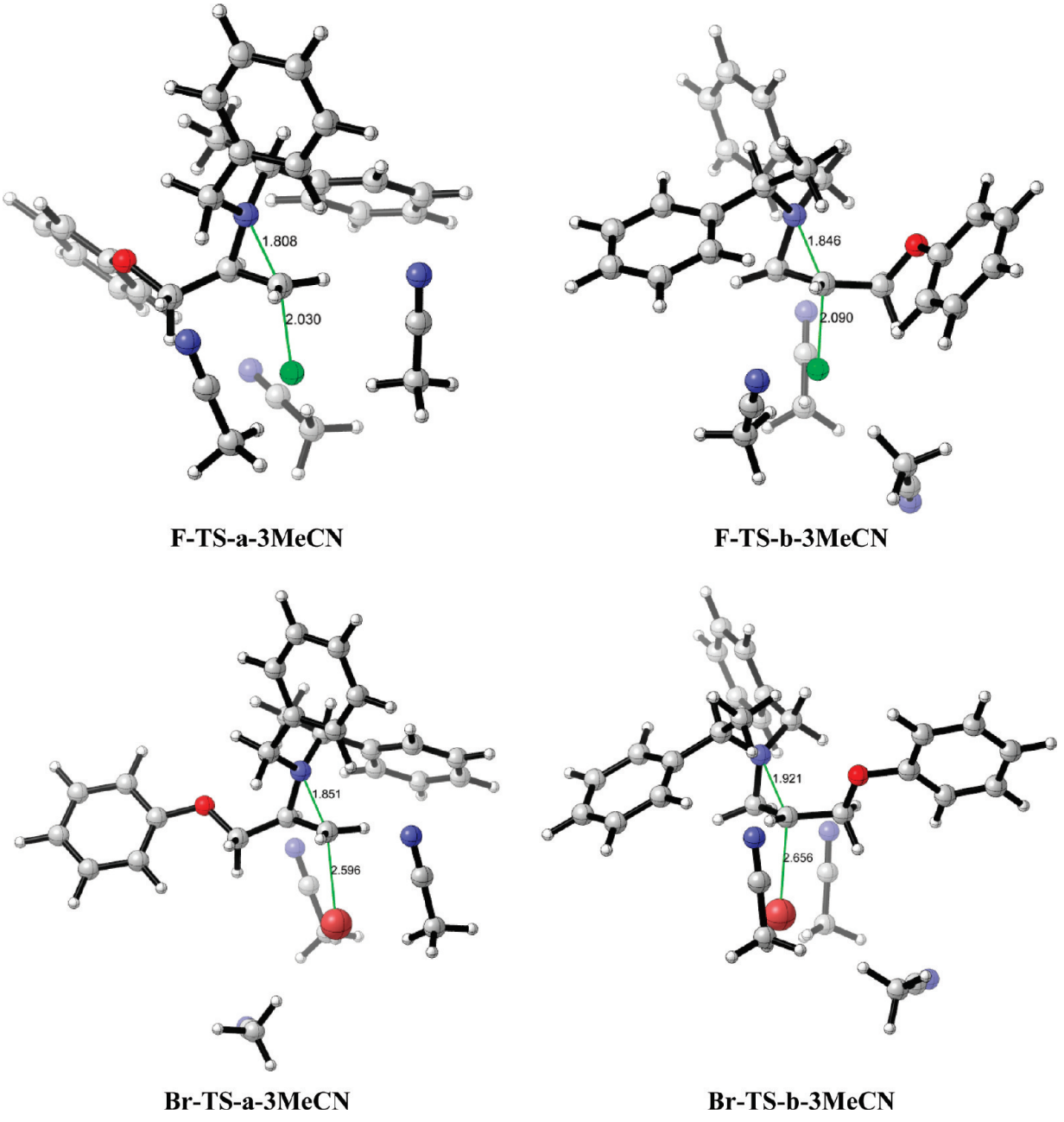

FIGURE 4. Transition state geometries optimized at the B3LYP/6-31++G(d,p) level of theory for halide-induced nucleophilic ring opening of aziridinium ion **12-T1**, with explicit solvent, through pathways a and b. Some critical distances (Å) are given.

will help elucidate the role of sterics and nucleophile strength on regioselectivity and the effect of solvating halide ions. Moreover, the dependence of the results on the level of theory used will be thoroughly discussed.

1. Hydrides. Transition state geometries for the S_N2 attack of BH_4^- and AlH_4^- on both aziridine carbons of **12-T1** are illustrated in Figure 2. Critical distances with respect to each pathway (C2−N for pathway a and C3−N for pathway b) are almost identical for both nucleophiles. All four transition states are early and have reactant-like structures; however, the difference in elongation along C3−N (1.724 Å for **AlH_4-TS-a**) and C2−N (1.792 Å for **AlH_4-TS-b**) is significant and indicative of the difference in progression along the reaction coordinate for pathways a and b. The fact that **TS-a** is an earlier transition state than **TS-b** already suggests that the barrier for pathway a will be slightly smaller than that for pathway b.

Relative energies along the reaction coordinate for the hydride-induced ring openings of aziridinium ions are given in Table 5. Calculations reveal a clear preference for pathway a for both hydride donating species, as depicted in the difference in relative energies of **TS-a** and **TS-b** at all levels of theory. Pathway a is shown to be the kinetically preferred route for hydride attack, hence confirming the experimentally observed regioselectivity. Relative stabilities of products also indicate that the kinetic product (**PC-a**) is incidentally the thermodynamically more stable one, indicating an Evans−Polanyi relation. Comparison of different

TABLE 6. Relative Electronic Energies (kJ/mol) of Stationary Points along the Reaction Coordinate for Nonsolvated Halide-Induced Nucleophilic Ring Opening of 12-T1 via Pathways a (Unhindered) and b (Hindered)[a,b]

	nonsolvated F^-					nonsolvated Br^-				
method	RC	TS-a	TS-b	P-a	P-b	RC	TS-a	TS-b	P-a	P-b
B3LYP/6-31++G(d,p)	0.0	63.9	62.7	−135.2	−134.7	0.0	8.9	14.2	−106.3	−115.7
B3LYP-D/6-31++G(d,p)	0.0	68.8	65.6	−126.6	−115.4	0.0	10.0	12.1	−99.5	−107.0
MPW1B95/6-31++G(d,p)	0.0	68.9	68.0	−134.3	−129.4	0.0	18.5	24.2	−97.8	−105.3
PBE0/6-31++G(d,p)	0.0	69.3	70.0	−136.9	−133.0	0.0	17.8	25.3	−102.7	−111.4
BMK/6-31++G(d,p)	0.0	67.9	67.4	−145.5	−138.2	0.0	14.8	19.8	−107.5	−114.3
MP2/6-31++G(d,p)	0.0	65.2	64.3	−123.4	−104.7	0.0	22.9	26.6	−86.1	−101.5
SCS-MP2/6-31++G(d,p)	0.0	62.1	61.1	−134.3	−118.5	0.0	21.5	26.3	−90.6	−105.6
B2-PLYP/TZVP	0.0	69.6	67.8	−141.0	−134.6	0.0	20.0	26.0	−94.2	−94.3

[a]RC, TS, and P represent reactive complex, transition state, and product, respectively. [b]B3LYP/6-31++G(d,p) geometries.

TABLE 7. Relative Electronic Energies (kJ/mol) of Stationary Points along the Reaction Coordinate for Solvated Halide-Induced Nucleophilic Ring Opening of 12-T1 via Pathways a (Unhindered) and b (Hindered)[a,b]

	solvated F^-					solvated Br^-				
method	RC	TS-a	TS-b	P-a	P-b	RC	TS-a	TS-b	P-a	P-b
B3LYP/6-31++G(d,p)	0.0	41.7	57.3	−79.8	−81.1	0.0	44.1	50.3	−11.9	−21.8
B3LYP-D/6-31++G(d,p)	0.0	40.2	60.8	−58.6	−48.8	0.0	47.2	50.4	1.8	−12.1
MPW1B95/6-31++G(d,p)	0.0	45.2	64.7	−80.7	−74.9	0.0	60.8	68.6	−2.6	−12.8
PBE0/6-31++G(d,p)	0.0	49.0	67.7	−77.8	−76.3	0.0	53.7	61.8	−8.9	−20.4
BMK/6-31++G(d,p)	0.0	42.4	62.1	−84.4	−77.4	0.0	52.3	60.9	−6.0	−22.0
MP2/6-31++G(d,p)	0.0	48.5	73.8	−56.4	−36.0	0.0	60.1	71.3	3.8	−13.6
SCS-MP2/6-31++G(d,p)	0.0	45.4	68.8	−72.0	−54.5	0.0	59.6	71.4	−3.1	−17.7

[a]RC, TS, and P represent reactive complex, transition state, and product, respectively. [b]B3LYP/6-31++G(d,p) geometries.

levels of theory indicates that the meta-hybrid GGA functional MPW1B95 effectively reproduces barrier heights that are consistent with MP2 and SCS-MP2, whereas B3LYP underestimates them by more than 10 kJ/mol.

2. Halides. As mentioned earlier, halide-induced ring openings for F^- and Br^- have been modeled *with* and *without* the use of explicit solvent molecules. These will be referred to as the solvated and nonsolvated cases, respectively. A previous theoretical study on ring opening with bromide has shown that coordination solvation energy converges with the inclusion of four explicit acetonitrile (MeCN) molecules;[14] however, the free energy of solvation is expected to converge earlier, due to the entropic penalty of adding additional solvent molecules. Therefore in the current study, three explicit acetonitrile molecules have been used to solvate the F^- and Br^- ions that attack the aziridinium ring. The solvated and nonsolvated cases will be comparatively analyzed to illustrate the benefit and necessity of solvating halide ions.

Transition state geometries for the S_N2 attack of nonsolvated F^- and Br^- on both aziridine carbons of **12-T1** are illustrated in Figure 3. Critical distances indicating ring opening within the aziridine and nucleophile-aziridine attack are considerably different in both pathways for both nucleophiles. Although halide−aziridine carbon distances are almost identical for both pathways in the bromide case, a considerable difference is observed among fluoride−aziridine carbon distances for pathways a and b (2.386 Å in **F-TS-a**, 2.248 Å in **F-TS-b**). It is also noteworthy to indicate that the C3−N bond distance (1.567 Å) in **F-TS-a** is only slightly longer than the C2−N bond distance (1.506 Å) in the reactant, indicating a very early transition state.

Transition state geometries for the S_N2 attack of solvated F^- and Br^- on **12-T1** are illustrated in Figure 4. Acetonitrile molecules stabilize the halide ions through charge-dipole interactions; typical $X\cdots H_3C-CN$ distances for fluoride and bromide are 2.0 and 2.7 Å, respectively. Critical distances are significantly different for the solvated versus nonsolvated halides in both pathways for both nucleophiles. Solvation has significantly changed the nature of the potential energy surface; whereas the nonsolvated cases show "reactant-like" transition states, the solvated ones are clearly "product-like". This is most pronounced in the extent of ring opening indicated by the C2−N and C3−N distances.

SCHEME 4. Thermodynamic Equilibration for Aziridinium Ring Opening with Bromide

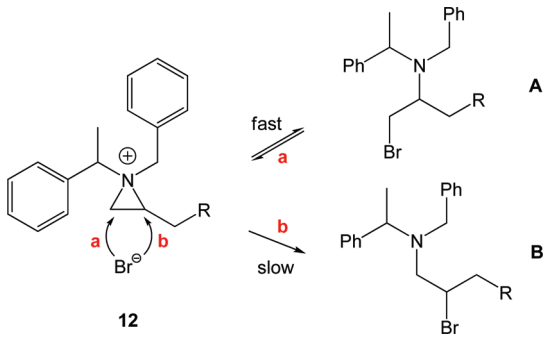

Relative energies along the reaction coordinate for the nonsolvated and solvated halide cases were calculated with a range of computational methods, as tabulated in Tables 6 and 7, respectively. An overall look at the relative stabilities of the reactive complex (**RC**), transition states (**TS-a** and **TS-b**), and products (**P-a** and **P-b**) for pathways a and b show quite a range of values for solvated versus bare ions. All levels of theory depict similar barriers for pathways a and b in the nonsolvated fluoride case. However, there is a remarkable barrier difference between the two pathways for fluoride attack in the solvated case, pointing toward the unhindered route, which also leads to the experimentally observed

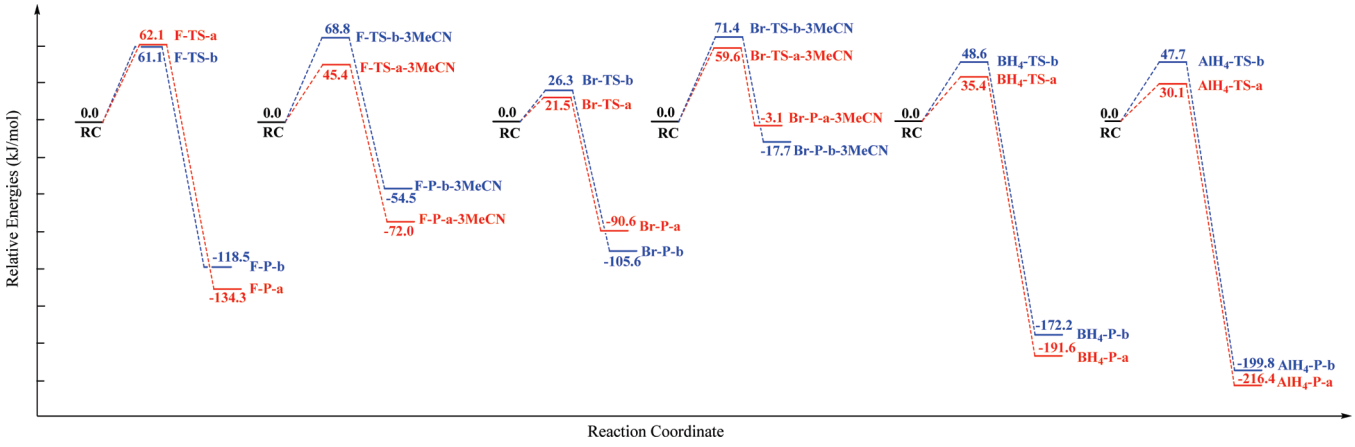

FIGURE 5. Potential energy surfaces (PESs) for the nucleophilic ring opening of **12-T1** with various nucleophiles (SCS-MP2/6-31++G(d,p))//B3LYP/6-31++G(d,p)). Relative energies are given in kJ/mol.

product. Relative product stabilities (**F-P-a** and **F-P-b**; **F-P-a-3MeCN**, and **F-P-b-3MeCN**) are rather similar for fluoride, in both nonsolvated and solvated cases. For the bromide, reaction barriers for both pathways are quite comparable, preventing a kinetic conclusion in both the nonsolvated and solvated case. However, product stabilities tend to favor pathway b, and therefore it is highly likely that the thermodynamic equilibration dictates the outcome of ring opening with bromide (Scheme 4). Although this can only occur if the barrier for the back reaction is feasible, in the nonsolvated case back reaction barriers are approximately 125 kJ/mol, i.e., too high for the reverse reaction to occur. However, this is merely an artifact of gas-phase calculations; extremely exothermic reaction energies are due to the fact that the bare halide ion is unrealistically stabilized in the product, whereas back reaction barriers are shown to be much lower in the solvated case, easily allowing equilibration to yield the more stable product. This is also in line with the fact that bromide is a soft nucleophile and a good leaving group, allowing thermodynamic equilibration.

Once again B3LYP underestimates barriers by approximately 10 kJ/mol (with nonsolvated fluoride being the exception), and dispersion corrections on B3LYP (B3LYP-D) energies do not show a remarkable improvement. On average, the meta-hybrid GGA functional MPW1B95 performs well in terms of barrier heights and reaction energies, showing remarkable correlation with SCS-MP2 energies. This also verifies the choice of functional in previous computational studies on ring opening of aziridinium ions by bromide.[12,14,17] In addition, this is in line with Bickelhaupt's report[59] on S_N2 benchmarks with different methodologies, which shows that GGA functionals, BLYP, PW91, and PBE dramatically underestimate S_N2 barriers, while hybrid functionals perform much better.

For a clearer picture, Figure 5 depicts potential energy surfaces (PESs) for all halides, solvated and nonsolvated, at the SCS-MP2//B3LYP/6-31++G(d,p) level of theory. In the nonsolvated fluoride case, **F-TS-a** and **F-TS-b** are virtually indistinguishable; both pathways (a and b) seem almost equally probable in terms of kinetics. However, this picture changes drastically in the presence of explicit solvation,

TABLE 8. Differences in Reaction Barriers ($\Delta\Delta E^{\ddagger}$), Distortion ($\Delta\Delta E^{\ddagger}_{dist}$), and Interaction Energies ($\Delta\Delta E^{\ddagger}_{int}$) (kJ/mol) between Pathways a and b for the Hydride- and Halide-Induced Nucleophilic Ring Opening of 12-T1[a,b]

	B3LYP/6-31++G(d,p)			MP2/6-31++G(d,p)		
	$\Delta\Delta E^{\ddagger}$	$\Delta\Delta E^{\ddagger}_{dist}$	$\Delta\Delta E^{\ddagger}_{int}$	$\Delta\Delta E^{\ddagger}$	$\Delta\Delta E^{\ddagger}_{dist}$	$\Delta\Delta E^{\ddagger}_{int}$
BH_4^-	13.1	16.7	−3.6	13.2	19.5	−6.3
AlH_4^-	14.4	20.0	−5.6	17.9	24.9	−7.0
nonsolvated F^-	−1.2	2.2	−3.4	−0.9	2.0	−2.9
nonsolvated Br^-	5.3	13.4	−8.1	3.7	13.2	−9.5
solvated F^-	15.6	0.9	14.7	25.3	9.3	16.0
solvated Br^-	6.2	8.9	−2.7	10.2	17.3	−7.1

[a] $\Delta\Delta E^{\ddagger} = \Delta E_b^{\ddagger} - \Delta E_a^{\ddagger}$. [b] B3LYP/6-31++G(d,p) geometries.

pathway a is favored over pathway b by an energy difference of approximately 20 kJ/mol, at all levels of theory. Accordingly, the energetically more favorable product, **F-P-a-3MeCN**, is incidentally also the experimentally observed one. The difference in relative energies between transition states is quite close for bromide, for solvated (**Br-TS-a-3MeCN** and **Br-TS-b-3MeCN**) and nonsolvated (**Br-TS-a** and **Br-TS-b**) cases, ruling out kinetic conclusions. It seems likely that bromide is less influenced by the difference in steric hindrance around the two aziridine carbons, since the bromide to aziridine-carbon distances are substantially larger than those for the fluoride; this is especially evident in the solvated case. From these results, it seems plausible to predict that in the absence of a large energy difference between transition states, the thermodynamically more favorable product is expected to form, if back reaction barriers are energetically feasible.[60]

Distortion/Interaction Model. Efforts to rationalize the experimentally observed reaction outcomes have also led to comparative analysis of the transition state structures via the distortion/interaction model.[61] To further verify the relationship between the structural distinctions and the difference in relative free energies of the transition states, the distortion/interaction model by Houk,[61−63] also known

(59) Bento, A. P. c.; Solà, M.; Bickelhaupt, F. M. *J. Chem. Theory Comput.* **2008**, *4*, 929.

(60) Sivaprakasham, M.; Couty, F.; Evano, G.; Srinivas, B.; Sridhar, R.; Rao, K. R. *Arkivoc* **2007**, *x*, 71.

(61) Ess, D. H.; Houk, K. N. *J. Am. Chem. Soc.* **2007**, *129*, 10646.

(62) Schoenebeck, F.; Ess, D. H.; Jones, G. O.; Houk, K. N. *J. Am. Chem. Soc.* **2009**, *131*, 8121.

(63) Ess, D. H.; Houk, K. N. *J. Am. Chem. Soc.* **2008**, *130*, 10187.

TABLE 9. Transition State (B3LYP/6-31++G(d,p)) Critical Distances (Å) and Bond Elongation Percentages for the Nitrogen-Aziridine Carbon Bond along the Reaction Coordinate for Pathways a (Unhindered) and b (Hindered)[a]

	pathway a			pathway b		
X	d(X−C3)	d(N−C3)	P(N−C3)[b] (%)	d(X−C2)	d(N−C2)	P(N−C2)[c] (%)
BH_4^-	1.956	1.726	15.4	1.970	1.796	19.3
AlH_4^-	1.997	1.724	15.2	2.016	1.792	19.0
nonsolvated F^-	2.386	1.567	4.7	2.248	1.664	10.5
nonsolvated Br^-	2.763	1.666	11.4	2.740	1.762	17.0
solvated F^-	2.030	1.808	20.9	2.090	1.846	22.6
solvated Br^-	2.596	1.851	23.7	2.656	1.921	27.6

[a]Bond elongation percentages P(N−C) (%) = $(d_{TS} - d_{reactant})/(d_{reactant})$. [b]$d(N-C3)_{reactant}$ = 1.496 Å from **12-T1** (B3LYP/6-31++G(d,p). [c]$d(N-C2)_{reactant}$ = 1.506 Å from **12-T1** (B3LYP/6-31++G(d,p).

as the activation strain model of chemical reactivity by Bickelhaupt,[64] was employed.

$$\Delta E^{\ddagger} = \Delta E^{\ddagger}_{dist} + \Delta E^{\ddagger}_{int}$$

The distortion/interaction model dissects the activation energy ($\Delta E^{\ddagger}$) into distortion energy ($\Delta E^{\ddagger}_{dist}$), and interaction energy ($\Delta E^{\ddagger}_{int}$) between distorted fragments, where the former is associated with the strain caused by deforming the individual reactants, and the latter is the favorable interaction between the deformed reactants. Fragment distortion and interaction energies at the B3LYP/6-31++G(d,p) and MP2/6-31++G(d,p) level of theory are given in Table 8.

For the halides, the distortion energy is shown to increase while going from fluoride to bromide in both the solvated and nonsolvated cases. The penalty for distorting the aziridinium ring is larger as the nucleophile gets larger; this is also reflected in the difference in elongation in the aziridinium ring (Figure 3) and is an indication of the difference in progression along the reaction coordinate; the transition state is more and more product-like as we go down the halide series. For the hydrides, the difference in activation energy is mainly caused by the difference in distortion, in line with the aforementioned structural differences in transition state geometries (Figure 2). Distortion/interaction calculations have revealed that the largest contribution to the difference in activation barriers comes from the strain caused by the deforming the reactants, while the difference in orbital interactions among competing pathways is shown to be relatively smaller, except for the solvated fluoride case, where the difference in interaction energies are noteworthy; the difference in energy barriers leading to the two competing pathways is almost exclusively due to the difference in interaction energies between the two transition states, indicating that the fluoride ion is much more influenced by the sterics around the aziridine carbon under attack (fluoride aziridine carbon distances in the transition state are approximately 2.0 Å, Figure 4). This is certainly not the case for bromide, which is considerably further away from the aziridinium moiety in the transition state (bromide aziridine carbon distances in the transition state are approximately 2.6 Å, Figure 4).

To obtain more insight into the reaction mechanism, the progression of some critical distances along the reaction coordinate has been studied.[65] For this purpose, both halide−aziridine carbon and nitrogen−aziridine carbon distances are tabulated in Table 9. Bond elongation percentages were calculated with respect to the parent aziridinium ion **12-T1**. Elongation percentages are higher by approximately 5% in pathway b for all nucleophiles; this is in line with the difference in distortion energies ($\Delta\Delta E^{\ddagger}_{dist}$) between the two pathways as tabulated earlier (Table 8). There is a remarkable difference in elongation percentages between the nonsolvated and solvated halides, once again illustrating the difference solvation has caused with respect to the progression along the reaction coordinate.

Conclusions

Nucleophilic ring opening of *N,N*-dibenzyl-2-substituted aziridinium ions at either of the aziridine ring carbons has been studied by means of computational methods in an attempt to rationalize experimentally observed regioselectivities. As the substrate bears aromatic units, various conformers, which differ by their stacking interactions, were identified. Only electronic levels of theory, taking into account dispersion interactions, were able to account for the parallel displaced conformers. However, the most stable reactant complex (**12-T1**) is characterized by T-stacking interactions and could be properly identified with DFT methods. Aziridinium ion **12-T1** has been analyzed in terms of susceptibility toward nucleophilic attack by hydride donating species (BH_4^- and AlH_4^-) and halides (F^- and Br^-). Explicit solvent molecules were used to solvate the halide ions, nonsolvated and solvated cases were comparatively discussed. The effect of solvation on the energetics of halide-induced ring-opening reactions of aziridinium ions is remarkable. Dramatic differences were observed between the two cases, and the necessity to solvate bare ions has become evident. A thorough level of theory study has shown that MPW1B95 is adequate for obtaining reliable barrier heights as well as reaction energies in the ring opening of aziridinium ions. In the hydride case, the kinetically viable route was shown to lead to the thermodynamically more stable product. For halides, the potential energy surface has drastically changed with solvation. While the differences in barriers were indistinguishable in the nonsolvated fluoride case, in the solvated case a clear kinetic preference for pathway a, correctly predicting the experimental result, was observed. In the bromide case, barriers showed no clear preference for either pathway; however, product stabilities seemed to dictate the outcome of the reaction through thermodynamic control, yet barriers for the back reaction were shown to be too high in the nonsolvated case, since the stabilization of the

(64) Bento, A. P.; Bickelhaupt, F. M. *J. Org. Chem.* **2008**, *73*, 7290.
(65) Van Speybroeck, V.; Martele, Y.; Waroquier, M.; Schacht, E. *J. Am. Chem. Soc.* **2001**, *123*, 10650.

halide ion was unrealistically reflected in the exothermicity of the reaction. The necessity to model halides with explicit solvation was shown through the significant decrease in exothermicity in the solvated case, leading to feasible barriers for the back reaction. Distortion/interaction analysis on the transition states has shown a major difference between pathways in terms of the extent of elongation and the progression along the reaction coordinate. Difference in barriers for the solvated fluoride case were shown to be mainly due to the difference in interaction energies, pointing to the fact that sterics dictates the outcome, whereas for bromide the difference in interaction energies are insignificant, suggesting that bromide is not effected by the difference in sterics, possibly since it is positioned significantly further away from the aziridine carbons at the transition state.

Acknowledgment. This work was supported by the Fund for Scientific Research-Flanders (FWO-Vlaanderen) and the Research Board of Ghent University (BOF). Computational resources and services used in this work were provided by Ghent University.

Supporting Information Available: Full refs 34 and 36, absolute energies and Cartesian coordinates of aziridinium conformers and transition states. This material is available free of charge via the Internet at http://pubs.acs.org.